JACS
JOURNAL OF THE AMERICAN CHEMICAL SOCIETY
Communication
pubs.acs.org/JACS

Positive Magneto-LC Effect in Conjugated Spin-Bearing Hexabenzocoronene

Prince Ravat, Tomasz Marszalek, Wojciech Pisula, Klaus Müllen, and Martin Baumgarten*

Max Planck Institute for Polymer Research, Ackermannweg-10, D-55128, Mainz, Germany

Supporting Information

ABSTRACT: The first neutral spin carrying hexabenzocoronene (HBC) derivative is described. The conjugated phenyl nitroxide substituted HBC with five alkyl chains exhibits a positive magneto-LC effect in columnar hexagonal liquid crystalline phase as probed by differential scanning calorimetry and electron paramagnetic resonance spectroscopy. Surprisingly, at 140 K the $\Delta M_S = 2$ transition can be observed indicating a thermally accessible triplet state between the neighboring molecules in the columnar arrangements.

Among the various discotics bearing large aromatic cores, hexa-peri-hexabenzocoronenes (HBCs) attracted particular attention because of their assembly into stable columnar structures and promising electronic properties.[1] HBCs have been functionalized with various substituents in order to steer their electronic properties and device applications.[2] Earlier studies have shown that HBCs or arylamine substituted HBCs can be reduced or oxidized to their corresponding radical anions and cations, respectively.[3] These radicals, however, could not be isolated as material in pure form owing to their limited stability and were only characterized by in situ analysis with electron paramagnetic resonance (EPR) and/or UV−vis spectroscopy. The peculiar ability of HBCs to arrange into columnar superstructures may allow one-dimensional magnetic ordering. Therefore, it was intriguing to design a spin-bearing HBC derivative and study its magnetic behavior in different crystalline phases. Moreover higher conductivity through the columns could be expected in spin-bearing HBCs in comparison to their closed-shell analogue because of the relatively high-lying singly occupied molecular orbital (SOMO) and its delocalization into the aromatic core.[4]

Herein, we report the synthesis and characterization of a neutral paramagnetic HBC derivative carrying a conjugated *tert*-butyl nitroxide radical moiety (HBCNO). The positive magneto-LC effect was observed by variable-temperature EPR spectroscopy in a columnar hexagonal liquid crystalline phase.

The precursor HBC-Br (2-bromo-5,8,11,14,17-pentadodecylhexabenzocoronene) was synthesized according to literature procedures.[5] The *tert*-butyldimethylsilyl-protected *N*-(*tert*-butyl)-*N*-phenylhydroxylamine was attached to HBC by Suzuki coupling reaction of HBC-Br with 4-(*tert*-butyl(*tert*-butyldimethylsilyloxy)amino)phenylboronicacid (4PBA) providing HBCSINO in 70% yield. The deprotection of *tert*-butyldimethylsilyl with aqueous HCl gave hydroxyl amine which was used further without any purification. Upon oxidation of hydroxyl amine with silver oxide the desired product HBCNO was obtained in 20% yield in two steps.

The phase transitions were identified by using differential scanning calorimetry (DSC) which exhibited three endothermic peaks during heating (Figure 1). The main peak (3) at 368

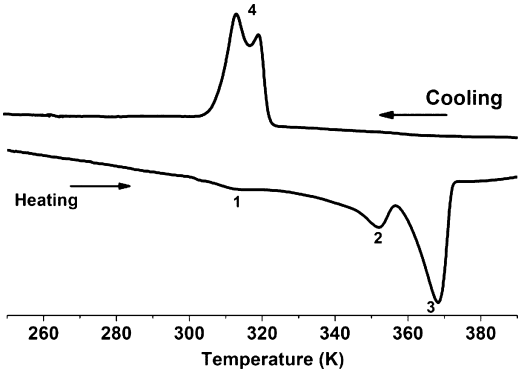

Figure 1. DSC plot of HBCNO (cooling and heating from 250 to 390 K) at a rate of 5 K min^{-1}.

K is related to the transition from a well-ordered helical columnar to the liquid crystalline phase. The detailed phase assignment is based on the structural analysis below. The minor peak (2) at 352 K prior the phase transition could stem from a cold crystallization. The small and broad transition (1) at 314 K is due to the reorganization of the side chains during heating. Upon cooling, a broad double peak (4) was observed which was related to two processes at close temperatures: the phase transition back to the ordered helical phase and crystallization of side chains.

To precisely assign the phases of HBCNO obtained during the DSC scans, the organization in bulk was studied by two-dimensional wide-angle X-ray scattering (2DWAXS) (Figure 2a). The structural investigation of the bulk supramolecular organization was performed on macroscopically aligned fibers prepared by mechanical extrusion. For the measurements, the fibers were mounted vertically toward the 2D detector which collected the scattered reflections. In our previous studies on discotic liquid crystals, this technique provided valuable information about the molecular arrangement and order within such superstructures.[6] The pattern of HBCNO recorded for the liquid crystalline phase at elevated temperatures exhibited a typical hexagonal columnar organization with nontilted discs

Received: July 22, 2014
Published: August 27, 2014

   dx.doi.org/10.1021/ja507421x | J. Am. Chem. Soc. 2014, 136, 12860−12863

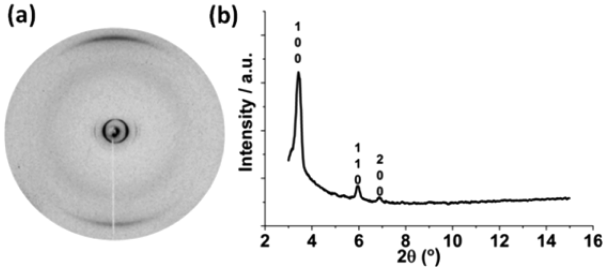

Figure 2. (a) 2DWAXS pattern of HBCNO (at 393 K) recorded in the liquid crystalline phase and (b) equatorial integration for HBCNO (reflections are assigned by Miller's indices).

(Figure 2). In the small-angle region, three sharp equatorial reflections were observed which correspond to the Miller's indices of 100, 110, and 200 for a hexagonal unit cell. The positions of the reflections are in the ratio of $1:\sqrt{3}:2$ confirmed the hexagonal lattice with an intercolumnar parameter of a_{hex} = 2.95 nm (Figure 2b). Wide-angle reflections in the meridional plane were attributed to the nontilted intracolumnar packing of the molecules from which a π-stacking distance of 0.35 nm for HBCNO was determined.

Upon cooling the compound back to the low-temperature phase (255 K), the supramolecular ordering significantly changed as evident from a high number of new and distinct reflections indicating a highly ordered phase (Figure 3a). In this

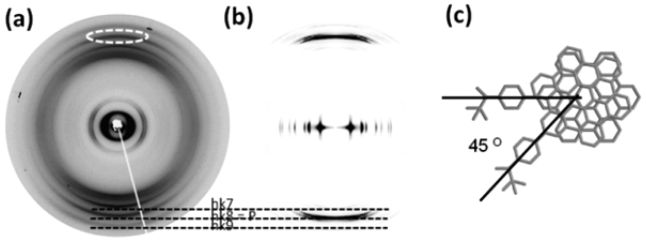

Figure 3. (a) 2DWAXS pattern of HBCNO recorded at 255 K in the low-temperature state after annealing in the LC phase. The scattering lines are assigned by Miller indices (*hkl* for l = 7, 8, 9) and indicate a characteristic helical intracolumnar organization. The *hkl* is a periodic reflection (P) assigned to π-stacking interaction indicated by dashed circle. (b) Cerius 2 simulation for a model based on helically packed nontilted HBC discs rotated by 45° toward each other leading to a helical repetition of 8 molecules, and (c) schematic illustration in top view of nontilted and 45° rotated HBCNO molecules.

phase the hexagonal lattice was maintained, but the unit cell parameter decreased to a_{hex} = 2.55 nm. At the same time, the π-stacking distance of the discs increased to 0.37 nm as determined from the most intensive wide-angle meridional reflection. Interestingly, additional meridional reflections in the wide-angle domain corresponding to *d*-spacings of 0.34 and 0.41 nm could be an evidence for a helical organization. From the even distribution of these meridional four reflections, a helical structure of 8 molecules was concluded, whereby the HBCNO molecules should be rotated by 45° toward each other (Figure 3c). Further reflections within the middle-range region related to the helical packing were missing. Cerius 2 simulations,[7] in which a HBC core was applied, confirm the described model yielding an X-ray pattern with the three characteristic reflections on the wide-angle meridional plane (Figure 3b). The disordered alkyl chains and the phenyl nitroxide are neglected in this model for simplicity. The simulated pattern also verified that off-meridional reflections in the middle-range region were missing, which otherwise would be typical for helical columnar structures. Most probably the phenyl nitroxide group was tilted with respect to the plane of the HBC core inducing a rotation of neighboring HBCNO discs and finally a helical arrangement within the columnar stack.

Thus, the 2DWAXS measurements gave important information about the molecular arrangement in the low and higher temperature phases. While at higher temperature the typical columnar hexagonal liquid crystalline (Col_h) phase was observed, in the lower temperature range the HBCNO molecules preferred to arrange in helical hexagonal crystalline (Hel_h) phase.

The solution EPR spectra of HBCNO were measured at room temperature in toluene at different concentrations. The diluted solution of HBCNO in toluene ($c \sim 10^{-5}$ M) yielded an EPR spectrum consisting of equally spaced 3 lines. The observed spectrum can be reproduced by spectral simulation considering *hfc* for one nitrogen a_N = 12.1 G and two equivalent protons a_H = 2 G at g-value 2.0068. Notably, at slightly higher concentration ($c \sim 10^{-4}$ M) the EPR spectrum was quite different and little alike a biradical species (Figure S1). This spectral change was due to the dimerization/aggregation of HBCNO molecules even at concentrations as low as 10^{-4} M. When the EPR spectrum of a powder sample was measured at 140 K, a broad resonance band was observed for ΔM_S = 1 transition with no fine structure splitting. Interestingly, along with a ΔM_S = 1 transition, at half field a forbidden ΔM_S = 2 transition was also observed at a *g*-value of 4.013 indicating the thermally accessible triplet state (Figure 4).

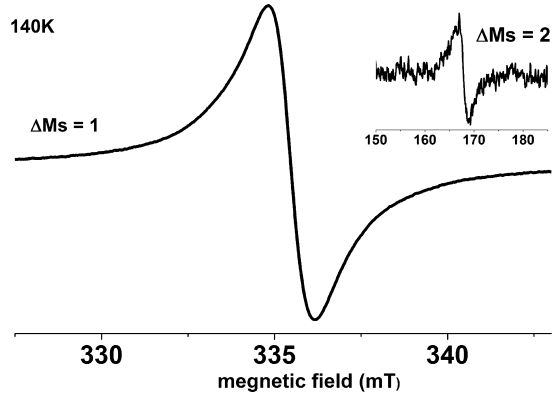

Figure 4. EPR spectra of HBCNO in solid state, ΔM_S = 1 and 2 transitions at 140 K.

Moreover EPR spectroscopy was found to be an excellent tool for probing the phase transition in spin bearing liquid crystals.[8] To obtain an insight into the change in magnetic interaction during phase transition, variable-temperature (VT) EPR spectra of a powder sample were measured during the cooling process in the temperature range 380 K (Col_h phase) to 270 K (Hel_h phase), and the variation of *g*-value, line intensity, and line width were plotted as a function of temperature. Very small changes in *g*-values from 2.0067 to 2.0070 were observed, indicating a minor variation in the orientation of the molecules during the transition from Col_h to Hel_h phase (Figure 5b). While the relative intensity and line width ($\Delta B_{1/2}$) remained nearly constant in the temperature range from 380 to 330 K, a sudden significant change of both parameters was observed at

dx.doi.org/10.1021/ja507421x | J. Am. Chem. Soc. 2014, 136, 12860−12863

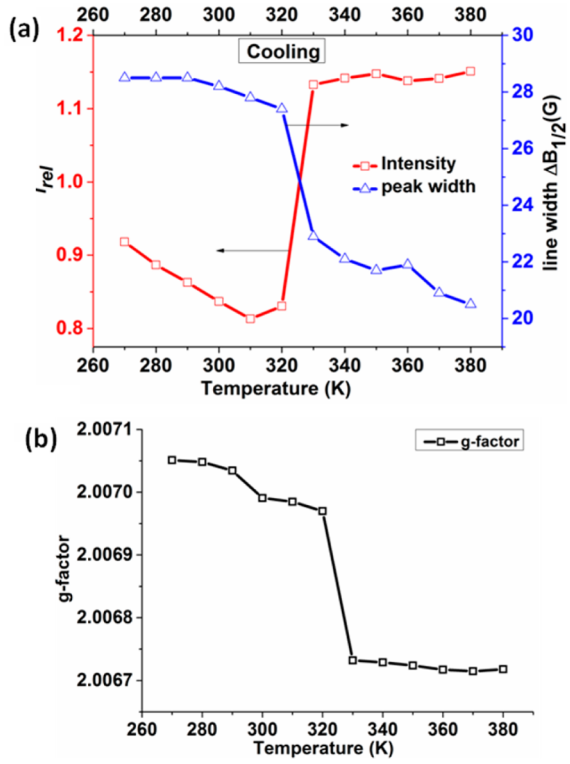

Figure 5. (a) Relative signal intensities and line widths and (b) *g*-factor during the cooling process as a function of temperature between 270 and 380 K.

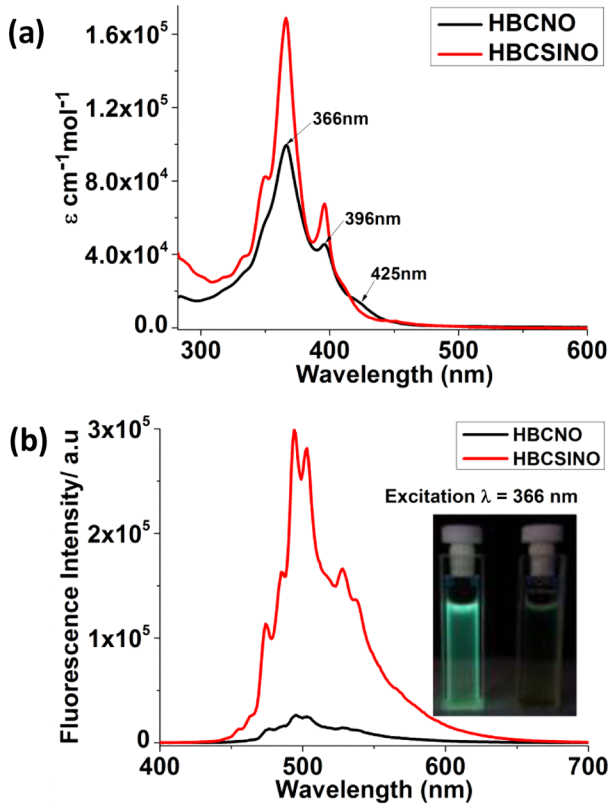

Figure 6. UV−vis spectrum of HBCSINO and HBCNO at room temperature in toluene (a) absorption (b) emission with excitation at 366 nm (inset: disappearance of fluorescence on conversion from HBCSINO (left fluorescent) to HBCNO (right nonfluorescent)).

320 K, i.e., at the onset of the phase transition (Figure 5a). A higher EPR signal intensity was detected in the Col_h phase as compared to the Hel_h phase indicating a positive magneto-LC effect ($J > 0$) in the Col_h phase. This was supported by 2DWAXS measurements which showed an enhanced π-stacking distance of the discs and the rotation of the HBCNO molecules during the phase transition from Col_h to Hel_h. In the temperature range from 310 to 270 K (Hel_h phase) the Curie law was obeyed, following the increase in intensity with decreasing temperature. The line width increased upon the phase transition from Col_h to Hel_h owing to the decrease in spin relaxation time. The increase of the line width in the Hel_h phase is attributed to a loss of the intracolumnar spin−spin exchange interaction during the transition from Col_h to Hel_h and can be corroborated with the positive magneto-LC effect in the Col_h phase. Such positive magneto-LC effect was also observed by Uchida et al. in chiral rod-like liquid crystalline nitroxide radical compounds.[8b,c] To the best of our knowledge this is the first example of spin bearing discotics exhibiting a positive magneto-LC effect.[9]

The optical measurements of HBCNO and precursor HBCSINO were performed in toluene ($c \sim 10^{-5}$ M) at room temperature. Interestingly, few notable changes were observed in the UV−vis spectra of HBCNO in comparison with HBCSINO. The β and *p*-bands of HBCNO were 1.5 times lower in intensity without any shift of λ_{max}. Additionally, the weak characteristic absorption of the radical moiety, which is due to the n—π^* transition, appeared as a shoulder of the *p*-band at 425 nm (Figure 6a). As anticipated for radical substituted aromatic compounds a dramatic quenching of the fluorescence was observed in HBCNO (Figure 6b).[10] This suggests the effective energy or electron transfer on excitation of HBCNO.[11]

The electrochemical properties of HBCNO were investigated by cyclic voltammetric (CV) measurements. CV scans of HBCNO displayed a reversible oxidation and a nonreversible reduction wave (Figure S2). The reversible oxidation at 0.269 V vs Fc/Fc^+ can be assigned to the oxidation of the nitroxide moiety which is in accordance with the literature value for nitroxides.[12] The DFT calculations were performed to visualize the distribution of the SOMO orbital, where the unpaired electron usually resides. As shown in Scheme 1, the SOMO orbital does not localize on the phenyl *tert*-butyl nitroxide radical moiety but is highly delocalized over the entire HBC core. The calculated SOMO energy level is well in accordance with the estimates from the CV measurement (Table S1).

In summary, we have successfully synthesized the first neutral paramagnetic HBC derivative possessing a *tert*-butyl nitroxide radical moiety. The adequate stability of HBCNO allowed us to investigate its thermal, optical, electrochemical, and magnetic properties. HBCNO was found to exist in a helical hexagonal phase at low temperature and a columnar hexagonal phase at higher temperatures. Notably, closer π-stacking of discs in the Col_h phase allowed stronger intracolumnar magnetic interactions. The paramagnetic HBCNO retains the absorption features of its diamagnetic precursor HBCSINO, but a significant quenching of fluorescence indicated extensive energy or electron transfer on excitation of HBCNO. All these properties make HBCNO an ideal candidate for designing spintronic devices.[8,13] Such work is underway in our group.

dx.doi.org/10.1021/ja507421x | J. Am. Chem. Soc. 2014, 136, 12860−12863

Scheme 1. Synthesis of HBCNO from HBC-Br

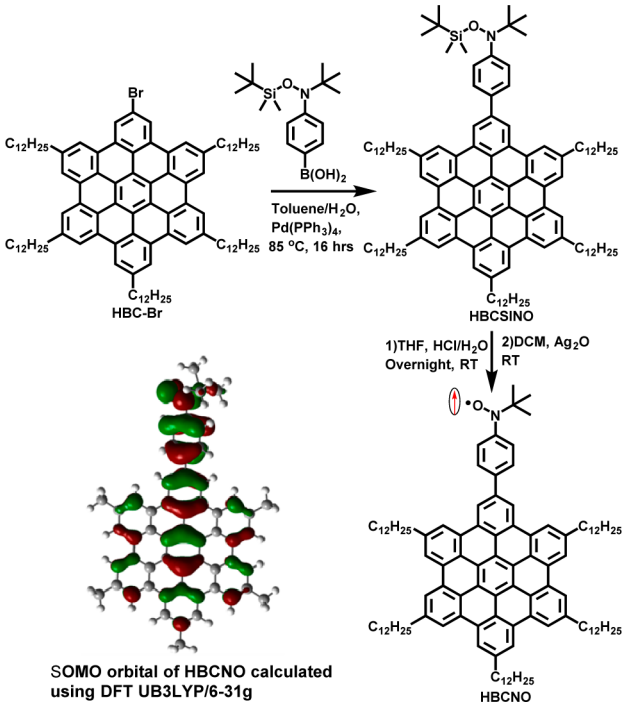

■ ASSOCIATED CONTENT

Supporting Information

Experimental procedure, EPR, NMR spectra and CV plot. This material is available free of charge via the Internet at http://pubs.acs.org.

■ AUTHOR INFORMATION

Corresponding Author

baumgart@mpip-mainz.mpg.de

Notes

The authors declare no competing financial interest.

■ ACKNOWLEDGMENTS

Support from SFB-TR49 and a scholarship for P.R. are gratefully acknowledged.

■ REFERENCES

(1) Schmidt-Mende, L.; Fechtenkötter, A.; Müllen, K.; Moons, E.; Friend, R. H.; MacKenzie, J. D. *Science* **2001**, *293*, 1119−1122.

(2) (a) Dössel, L. F.; Kamm, V.; Howard, I. A.; Laquai, F.; Pisula, W.; Feng, X.; Li, C.; Takase, M.; Kudernac, T.; De Feyter, S.; Müllen, K. *J. Am. Chem. Soc.* **2012**, *134*, 5876−5886. (b) Chen, L.; Dou, X.; Pisula, W.; Yang, X.; Wu, D.; Floudas, G.; Feng, X.; Müllen, K. *Chem. Commun.* **2012**, *48*, 702−704. (c) Wong, W. W. H.; Singh, T. B.; Vak, D.; Pisula, W.; Yan, C.; Feng, X.; Williams, E. L.; Chan, K. L.; Mao, Q.; Jones, D. J.; Ma, C.-Q.; Müllen, K.; Bäuerle, P.; Holmes, A. B. *Adv. Funct. Mater.* **2010**, *20*, 927−938. (d) Lucas, N. T.; Zareie, H. M.; McDonagh, A. M. *ACS Nano* **2007**, *1*, 348−354.

(3) (a) Wu, J. S.; Baumgarten, M.; Debije, M. G.; Warman, J. M.; Müllen, K. *Angew. Chem., Int. Ed.* **2004**, *43*, 5331−5335. (b) Gherghel, L.; Brand, J. D.; Baumgarten, M.; Müllen, K. *J. Am. Chem. Soc.* **1999**, *121*, 8104−8105.

(4) (a) Jankowiak, A.; Pociecha, D.; Szczytko, J.; Monobe, H.; Kaszyński, P. *J. Am. Chem. Soc.* **2012**, *134*, 2465−2468. (b) Jankowiak, A.; Pociecha, D.; Monobe, H.; Szczytko, J.; Kaszynski, P. *Chem. Commun.* **2012**, *48*, 7064−7066.

(5) (a) Ito, S.; Wehmeier, M.; Brand, J. D.; Kübel, C.; Epsch, R.; Rabe, J. P.; Müllen, K. *Chem.—Eur. J.* **2000**, *6*, 4327−4342. (b) Fechtenkötter, A.; Tchebotareva, N.; Watson, M.; Müllen, K. *Tetrahedron* **2001**, *57*, 3769−3783.

(6) Grigoriadis, C.; Haase, N.; Butt, H.-J.; Müllen, K.; Floudas, G. *Soft Matter* **2011**, *7*, 4680−4689.

(7) *Cerius 2* calculation; Accelrys, Inc.: San Diego, CA, 1998.

(8) (a) Castellanos, S.; López-Calahorra, F.; Brillas, E.; Juliá, L.; Velasco, D. *Angew. Chem., Int. Ed.* **2009**, *48*, 6516−6519. (b) Suzuki, K.; Uchida, Y.; Tamura, R.; Shimono, S.; Yamauchi, J. *J. Mater. Chem.* **2012**, *22*, 6799−6806. (c) Uchida, Y.; Suzuki, K.; Tamura, R.; Ikuma, N.; Shimono, S.; Noda, Y.; Yamauchi, J. *J. Am. Chem. Soc.* **2010**, *132*, 9746−9752.

(9) (a) Gopee, H.; Cammidge, A. N.; Oganesyan, V. S. *Angew. Chem., Int. Ed.* **2013**, *52*, 8917−8920. (b) Yelamaggad, C. V.; Achalkumar, A. S.; Rao, D. S. S.; Nobusawa, M.; Akutsu, H.; Yamada, J.-i.; Nakatsuji, S. i. *J. Mater. Chem.* **2008**, *18*, 3433−3437.

(10) Borozdina, Y. B.; Kamm, V.; Laquai, F.; Baumgarten, M. *J. Mater. Chem.* **2012**, *22*, 13260−13267.

(11) Ito, A.; Shimizu, A.; Kishida, N.; Kawanaka, Y.; Kosumi, D.; Hashimoto, H.; Teki, Y. *Angew. Chem., Int. Ed.* **2014**, *53*, 6715−6719.

(12) Kadirov, M.; Tretyakov, E.; Budnikova, Y.; Valitov, M.; Holin, K.; Gryaznova, T.; Ovcharenko, V.; Sinyashin, O. *J. Electroanal. Chem.* **2008**, *624*, 69−72.

(13) (a) Misiorny, M.; Hell, M.; Wegewijs, M. R. *Nat. Phys.* **2013**, *9*, 801−805. (b) Sugawara, T.; Matsushita, M. M. *J. Mater. Chem.* **2009**, *19*, 1738−1753.